PAPER • OPEN ACCESS

Comparison of the superconducting properties of Y-Ba-Cu-O and Y-Ba-Cu-O-Ag bulk superconductors

To cite this article: J V J Congreve *et al* 2019 *IOP Conf. Ser.: Mater. Sci. Eng.* **502** 012181

View the article online for updates and enhancements.

IOP ebooks™

Bringing you innovative digital publishing with leading voices to create your essential collection of books in STEM research.

Start exploring the collection - download the first chapter of every title for free.

Comparison of the superconducting properties of Y-Ba-Cu-O and Y-Ba-Cu-O-Ag bulk superconductors

J V J Congreve, Y H Shi, A R Dennis, J H Durrell and D A Cardwell

Department of Engineering, University of Cambridge, CB2 1PA, U.K.

Email: jvjc2@cam.ac.uk

Abstract The widespread use of RE-Ba-Cu-O [(RE)BCO] bulk superconductors, where RE=Y, Gd or Sm, in practical applications requires large single grains that exhibit uniform superconducting properties. Until recently, however, it was difficult to grow successfully YBCO-Ag bulk materials in the required single grain form, due primarily to the relative complexity of the top seeded melt growth process (TSMG) and the introduction of an alloying element (Ag) to the precursor composition. In most cases, alloying elements are used to improve the mechanical properties of the bulk superconductor whilst, at the same time, aim to cause minimal detrimental effect on the superconducting properties of the fully processed sample. In this work we investigate the effect of the addition of silver to YBCO on the superconducting properties of the bulk single grain, including trapped field, T_c and J_c, and on the sample microstructure.

1. Introduction

Single grain RE-Ba-Cu-O [(RE)BCO] bulk high temperature superconductors, where RE = Y, Gd or Sm, are able to trap significantly larger magnetic fields than those generated by permanent magnets [1, 2]. This enables this unique class of material to find practical application in a wide range of technologies, including Maglev trains, energy storage systems, rotating electrical machines and trapped flux devices [3-5].

(RE)BCO bulk superconductors are inherently brittle in nature (they are often described as ceramic-like), with their poor mechanical properties typically limiting the extent to which their superconducting properties can be exploited, especially at high fields [6, 7]. The addition of silver to (RE)BCO improves significantly the fracture toughness and bending strength of the bulk sample [8-10] and, unlike many other alloying elements, does not appear to degrade the superconducting properties of the single grain [11-13].

(RE)BCO superconductors for practical applications must be produced in the form of single grains to avoid the formation of grain boundaries, which strongly suppress critical current [14, 15], and limit severely the ability of this material to generate large magnetic fields. Following significant research over the past thirty years on the fabrication of (RE)BCO in the form of large single grains [16, 17], the so-called top seeded melt growth technique (TSMG) is now used routinely to fabricate large single grains of a wide range of (RE)BCO bulk superconductor compositions [14, 18]. This process involves heating the compacted precursor powder to the peritectic decomposition temperature to enable the superconducting $YBa_2Cu_3O_{7-\delta}$ (Y-123) phase to decompose into a secondary, non-superconducting Y_2BaCuO_5 (Y-211) solid phase and a residual Ba-Cu-O liquid phase. Slow, controlled undercooling in the presence of a suitable solid seed crystal then enables the nucleation and growth of a large single grain consisting of a continuous, superconducting Y-123 phase matrix containing a distribution of discrete, non-superconducting embedded Y-211 phase inclusions [14, 19].

Although the TSMG technique is one of the simplest fabrication techniques for these materials, it is based on the optimisation of many inter-dependent processing parameters and variables. In consequence, the addition of alloying elements complicates greatly the determination of the optimum processing conditions, and, indeed, whether or not a single grain can be grown successfully at all. The addition of silver changes the peritectic decomposition temperature of the precursor composition, although the element itself is, however, very stable chemically within the Y-123 phase matrix [20]. Recent developments in melt processing have led to the ability to grow large single grains of YBCO-Ag reliably and reproducibly. In order for these single grains to be of practical use, however, their superconducting properties must be of a comparable standard to those of standard YBCO fabricated by TSMG.

We report the use of liquid-phase enriched TSMG technique [21] to grow reliably large single grains of YBCO-Ag bulk superconductor [22]. The trapped field at the top and bottom surfaces of YBCO-Ag and YBCO single grains grown by TSMG have been compared with the measured distribution of T_c and J_c along the c-axis

of the samples. These data have, in turn, been compared with the microstructure and distribution of silver, where relevant, in order to establish the effect of silver and the microstructural features on the observed superconducting properties of the single grain in an attempt to identify the significance of the addition of this alloying element to the TSMG process.

2. Experimental Method

2.1 Sample fabrication

Four samples of YBCO of standard composition were grown by TSMG. Precursor powder was prepared from a mixture of 99.9% purity powders of Y-123:Y-211:CeO_2 in a mass ratio of 150:50:1. Pellets were pressed uniaxially from 46 g of precursor powder using a 30 mm diameter die. The curved edges and the bases of the cylindrical pellets were painted with a Yb_2O_3 paste and placed onto ZrO_2 rods on a ceramic plate. A buffer pellet [23-26] pressed uniaxially from 0.15g of precursor powder in a 5 mm diameter cylindrical die was placed at the centre of the top surface of each powder pellet, with a generic seed [27] placed, in turn, at the centre of the upper surface of the buffer pellet. Each sample was heated in a box furnace according to the heating profile shown in figure 1b.

Four samples of YBCO-Ag were grown by a liquid phase enriched TSMG technique [22]. Precursor powder was prepared from a mixture of 99.9% purity powders of Y-123:Y-211:CeO_2:Ag_2O in a mass ratio of 150:50:1:20. A liquid-phase-rich powder prepared from Yb_2O_3:$Ba_3Cu_5O_8$:BaO_2 in the ratio 5.0:5.6:1.0 was calcined at 850 °C for 5 hours. Powder pellets consisting of a 4.62 g layer of liquid-rich powder located below 46 g of silver-containing precursor powder were pressed uniaxially in a 30 mm diameter die. Painting of the sample edges and assembly of the buffer layer and generic seed crystal was carried out as described above for the sample processed without Ag. The assembly was heated according to the heating profile in figure 1a.

All samples were annealed in a tube furnace in an oxygen-rich atmosphere following melt processing. The samples were held at 450 °C for 8 days to enable the Y-123 matrix to transform fully from a tetragonal structure to a superconducting orthorhombic structure.
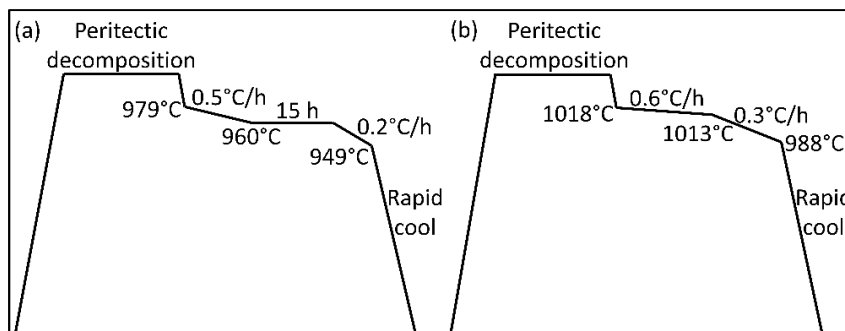

Figure 1 : Heating profiles for growth of: (a) YBCO-Ag by liquid-phase enriched TSMG, (b) YBCO by TSMG
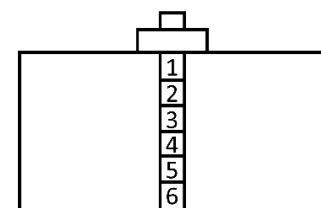

Figure 2: Schematic illustration of the sub-specimens cut from each single grain

2.2 Measurement of superconducting properties

The top and base of each as-processed sample was polished flat and parallel. The maximum trapped magnetic field at the top and bottom surfaces was measured using a hand held Hall probe positioned 0.5 mm from the surface following field cooling at 77 K in an applied magnetic field of 1.4 T. Trapped field profiles across the top and bottom surfaces of each single grain were measured using a rotating array of 20 Hall probes at a distance 1.0 ± 0.5 mm above the surface of each sample.

The four samples of YBCO and four samples of YBCO-Ag were cut in half along a diameter to expose a rectangular cross sectional area. A further slice was cut from one of each type of sample, chosen at random, and

then divided further into sub-specimens of approximate dimensions 1.5 mm x 2.0 mm x 1.2 mm, as shown schematically figure 2. The magnetic moment of each sample was measured using a SQUID (superconducting magnetic interference device) magnetometer (Quantum Design MPMS XL). The value of T_c was established directly from the measured data at a constant magnetic field of 1.6×10^3 A/m and the value of J_c at 77 K was derived from the magnetic hysteresis loops using the extended Bean model [28].

2.3 Microstructure and composition analysis

One half of the single grain samples was polished for microstructural evaluation. The samples were imaged using an optical microscope at 50 x magnification in order to view the pore and, where relevant, silver distribution within the bulk microstructure. Images were taken at 1 mm intervals along the central c-axis. ImageJ software [29] was used to determine the area fraction occupied by pores and, where relevant, silver agglomerates for each image. The colour threshold was adjusted to highlight the pores or silver agglomerates in a given image, with the "analyze particles" tool used to collect data on the size and area of the image occupied by these pores or agglomerates. Images were taken at intervals corresponding approximately to the location of the centre of each of the sub-specimens from the other half of the same sample used to measure T_c and J_c.

3. Results and discussion

3.1 Superconducting properties

All samples exhibited a trapped field profile with a single peak and a smooth, continuously decreasing radial field gradient, characteristic of a single grain sample. The average maximum trapped field and the maximum variation in trapped field between each sample is shown in figure 3. The average maximum trapped fields are almost identical for both sets of samples. There is, however, a greater variation in the range of maximum trapped field for YBCO-Ag than for YBCO, with the maximum trapped field at the top of one of the YBCO-Ag samples being 0.052 T higher than the absolute maximum trapped field recorded at the top of any of the standard YBCO samples.

The values of onset T_c were measured for sub-specimens along the central c-axis, numbered as shown in figure 2, and the ΔT value calculated (i.e. the temperature range over which the magnetic moment reduces by 90%, and hence a measure of the sharpness of transition). The values of T_c and ΔT are shown in Table 1. The value of T_c was a minimum of 0.2 K higher in the YBCO-Ag sample than in the YBCO sample for every corresponding sub-specimen. The transition to the superconducting state was also sharper for sub-specimens of YBCO-Ag than YBCO, with the exception of 2 equivalent samples.

The T_c values from each sub-specimen within each sample are very similar; these range between 91.0 K and 91.5 K or 91.5 K and 92.0 K in the YBCO and YBCO-Ag samples respectively. In addition the transition to superconducting (given by ΔT) is very sharp for all sub-specimens with the exception of the two sub-specimen fives. All sub-specimens, except these two, have a ΔT value of below 1.9 K.

The values of $J_c(0)$ for each sub-specimen are shown in Table 1. The initial part of each $J_c - B$ curve is approximately linear, which is why the $J_c(0)$ value has been recorded, as shown in figure 5. The highest value of $J_c(0)$ occurs at the centre of each sample, with the largest overall maximum observed in the YBCO-Ag sample. The values of J_c from each sub-specimen are very different, even for sub-specimens from the same sample. This value is generally found to vary between locations within the same sample. In addition, sub-specimens 1-3 of YBCO-Ag exhibit significantly higher values of $J_c(0)$ than those of the corresponding sub-specimens of YBCO. However, the values of J_c measured at the base of the samples were significantly and consistently higher in the YBCO sub-specimens.

3.2 Microstructural analysis

The central c-axis of each half single grain was imaged at 50 x magnification at intervals of 1 mm. Images were also taken at locations corresponding approximately to the centres of the sub-specimens cut from the

complementary half of the single grain, as shown in figure 4. The black, circular regions in these images correspond to pores, the black lines to cracks, the light yellow region to the Y-123 matrix containing Y-211 agglomerates and the bright yellow regions in the YBCO-Ag sample to silver agglomerates. These images show that the YBCO sample contains a much larger concentration of pores and cracks than the YBCO-Ag sample (this was observed consistently for all 8 samples). The distribution of pores and silver is very similar from sample-to-sample of the same type. The distribution and size of the silver agglomerates vary along the *c*-axis of the YBCO-Ag samples, with both large and small agglomerates present within the same image. The shape of the silver agglomerates and their proximity to pores indicates clearly that some of the Ag fills some of the pores. The area fraction occupied
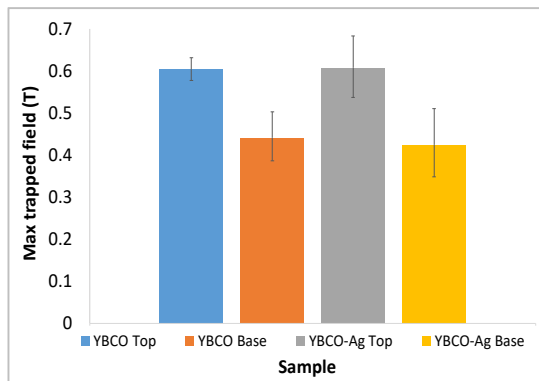

Figure 3: Maximum trapped field at the top and base of the samples. Error bars extend to the highest and lowest maximum trapped field recorded in the 8 samples

Table 1: Superconducting properties of YBCO and YBCO-Ag

Sub-specimen	YBCO			YBCO-Ag		
	T_c (K)	ΔT	$J_c(0)$ (A/cm^2)	T_c (K)	ΔT	$J_c(0)$ (A/cm^2)
1	91.0	1.2	39435	91.8	1.2	41653
2	91.5	1.1	41278	92.0	0.7	46468
3	91.5	1.1	45419	91.8	0.5	49477
4	91.5	0.8	41150	91.8	1.9	15995
5	91.3	3.7	26734	91.5	3.0	14474
6	91.3	0.7	40081	91.5	1.7	28665

by pores and silver in each of these images is shown in figure 6. There is a large variation in the porosity and a much larger fraction of area occupied by pores in the YBCO sample compared to the YBCO-Ag sample. This provides further evidence that the silver does, indeed, fill some of the pores.
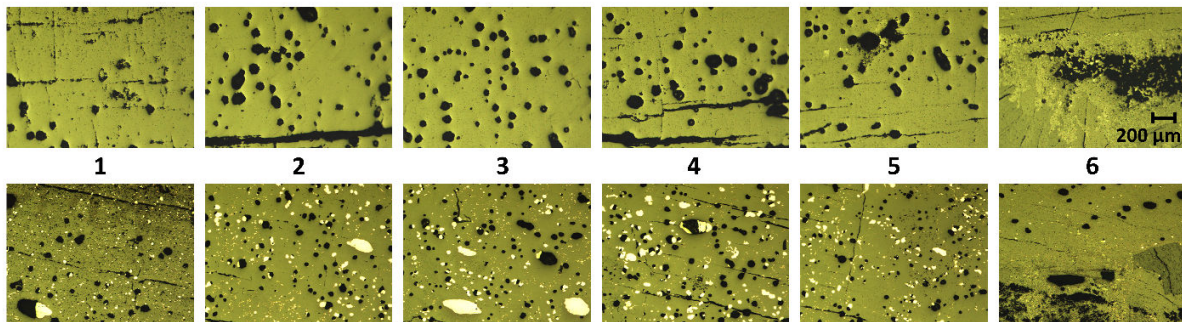

Figure 4: Microstructure at 50x magnification (top) YBCO, (bottom) YBCO-Ag for the different sub-specimen positions

3.3 Relation between composition and superconducting properties

Figure 6 shows the porosity and, where relevant, the silver distribution corresponding approximately to the location of each sub-specimen. These graphs confirm that the porosity is higher in the YBCO samples than in the YBCO-Ag samples. It is a concern that addition of silver may increase the proportion of the non-superconducting material present, given that neither the silver nor the pore regions are superconducting, and hence reduce J_c and trapped field. However, the average of the area occupied by silver and pores combined across the 6 locations in the YBCO-Ag sample was 12.5 % (this was calculated by summing the average area occupied by pores and the average area occupied by silver in each individual image and then finding the average percentage across all six images), whereas in the YBCO sample the average total area occupied by pores was slightly lower at 9.6 %. These averages include both cracks and pores and, where relevant, all sizes of silver agglomerates,

therefore, if there are large cracks present in one image or a large area fraction of pores or silver agglomerates these values will be affected significantly by the particular image in question. The total area fraction occupied by these non-superconducting regions does not seem to correlate with the J_c value for any given sub-specimen.
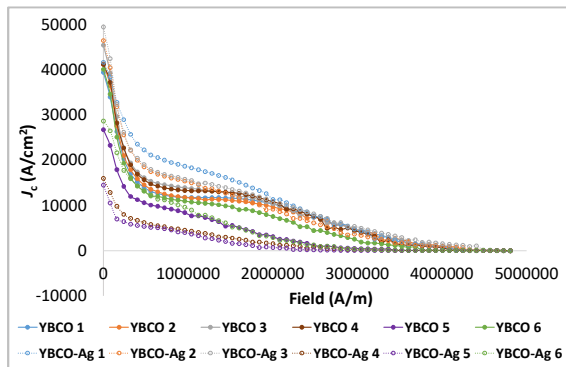

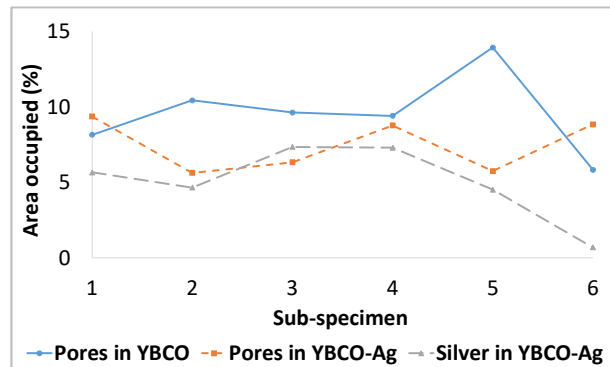Figure 5: J_c curves of all sub-specimens measured

Figure 6: Porosity and silver content in each sub-specimen

4. Conclusions

It has been demonstrated that the addition of silver to the YBCO system does not have a detrimental effect on the superconducting properties of single grains grown by the TSMG processing technique. YBCO-Ag single grains exhibit superconducting properties that are at least comparable to those of standard YBCO single grains, with the additional potential of improved mechanical properties. The trapped field properties of the YBCO-Ag single grains were higher in all cases, exhibiting the highest J_c and T_c and the sharpest transition to the superconducting state. In addition, the effect of the microstructure and the addition of silver have been studied and the relationship between J_c and porosity and silver content observed. Silver has been observed to fill many of the pores, which would have otherwise have been present in a standard YBCO single grain sample. The absence of any degradation in the superconducting properties of the YBCO system when Ag is added to the precursor composition suggests that this alloying element can lead to an improvement in the potential of YBCO-Ag for use in practical applications.

Acknowledgements

References

[1]   Durrell J H, Dennis A R, Jaroszynski J, Ainslie M D, Palmer K G B, Shi Y H, Campbell A M, Hull J, Strasik M, Hellstrom E E and Cardwell D A 2014 A trapped field of 17.6T in melt-processed, bulk Gd-Ba-Cu-O reinforced with shrink-fit steel *Supercond. Sci. Technol.* **27**

[2]   Zhai W, Shi Y H, Durrell J H, Dennis A R and Cardwell D A 2014 The Influence of Y-211 Content on the Growth Rate and Y-211 Distribution in Y-Ba-Cu-O Single Grains Fabricated by Top Seeded Melt Growth *Crystal Growth & Design* **14** 6367-75

[3]   Campbell A M and Cardwell D A 1997 Bulk high temperature superconductors for magnet applications *Cryogenics* **37** 567-75

[4]   Werfel F N, Floegel-Delor U, Rothfeld R, Riedel T, Goebel B, Wippich D and Schirrmeister P 2012 Superconductor bearings, flywheels and transportation *Supercond. Sci. Technol.* **25**

[5]   Li B Z, Zhou D F, Xu K, Hara S, Tsuzuki K, Miki M, Felder B, Deng Z G and Izumi M 2012 Materials process and applications of single grain (RE)-Ba-Cu-O bulk high-temperature superconductors *Physica C* **482** 50-7

[6]   Nishio T, Itoh Y, Ogasawara F, Suganuma M, Yamada Y and Mizutani U 1989 SUPERCONDUCTING AND MECHANICAL-PROPERTIES OF YBCO-AG COMPOSITE SUPERCONDUCTORS *Journal of Materials Science* **24** 3228-34

[7]   Iida K, Babu N H, Shi Y H, Miyazaki T, Sakai N, Murakami M and Cardwell D A 2008 *8th European Conference on Applied Superconductivity,* ed S Hoste and M Ausloos (Bristol: Iop Publishing Ltd)

[8]   Yeh F and White K W 1991 FRACTURE-TOUGHNESS BEHAVIOR OF THE YBA2CU3O7-X SUPERCONDUCTING CERAMIC WITH SILVER-OXIDE ADDITIONS *Journal of Applied Physics* **70** 4989-94

[9]   Diko P, Krabbes G and Wende C 2001 Influence of Ag addition on crystallization and microstructure of melt-grown single-grain YBa2Cu3O7 bulk superconductors *Supercond. Sci. Technol.* **14** 486-95

[10]   Nakamura Y, Tachibana K and Fujimoto H 1998 Dispersion of silver in the melt grown YBa2Cu3O6+x crystal *Physica C: Superconductivity* **306** 259-70

[11]   Azambuja P d, Rodrigues Jãºnior P, Jurelo A R, Serbena F C, Foerster C E n, Costa R n M, Souza G B d, Lepienski C M c and Chinelatto A L 2009 Effects of Ag addition on some physical properties of granular YBa2Cu3O7-´ superconductor *Brazilian Journal of Physics* **39** 638-44

[12]   Mendoza E, Puig T, Varesi E, Carrillo A E, Plain J and Obradors X 2000 Critical current enhancement in YBCO–Ag melt-textured composites: influence of microcrack density *Physica C: Superconductivity* **334** 7-14

[13]   Matsui M, Sakai N and Murakami M 2002 Effect of Ag 2 O addition on the trapped fields and mechanical properties of Nd–Ba–Cu–O bulk superconductors *Superconductor Science and Technology* **15** 1092

[14]   Cardwell D A 1998 Processing and properties of large grain (RE)BCO *Materials Science and Engineering B-Solid State Materials for Advanced Technology* **53** 1-10

[15]   1997 Crystal growth of bulk high-Tc superconducting oxide materials *Mater. Sci. Eng.* **19** 1

[16]   Dimos D, Chaudhari P, Mannhart J and Legoues F K 1988 ORIENTATION DEPENDENCE OF GRAIN-BOUNDARY CRITICAL CURRENTS IN YBA2CU3O7-DELTA BICRYSTALS *Physical Review Letters* **61** 219-22

[17]   Durrell J H, Hogg M J, Kahlmann F, Barber Z H, Blamire M G and Evetts J E 2003 Critical current of YBa2Cu3O7-delta low-angle grain boundaries *Physical Review Letters* **90**

[18]   Sawano K, Morita M, Tanaka M, Sasaki T, Kimura K, Takebayashi S, Kimura M and Miyamoto K 1991 HIGH MAGNETIC-FLUX TRAPPING BY MELT-GROWN YBACUO SUPERCONDUCTORS *Japanese Journal of Applied Physics Part 2-Letters* **30** L1157-L9

[19]   1990 Melt processing of YBaCuO oxide superconductors *Advances in Superconductivity: II. Proceedings of the 2nd International Symposium on Superconductivity* 285

[20]   Nakamura Y, Tachibana K, Kato S, Ban T, Yoo S I and Fujimoto H 1998 Phase relation in Y211-Y123-Ag system and morphology of silver in Y123 crystal *Physica C: Superconductivity and its Applications* **294** 302-15

[21]   Congreve J V J, Shi Y H, Dennis A R, Durrell J H and Cardwell D A 2017 Improvements in the processing of large grain, bulk Y-Ba-Cu-O superconductors via the use of additional liquid phase *Supercond. Sci. Technol.* **30** 11

[22]   Congreve J V J, Shi Y H, Dennis A R, Durrell J H and Cardwell D A 2018 The successful incorporation of Ag into single grain, Y-Ba-Cu-O bulk superconductors *Supercond. Sci. Technol.* **31** 7

[23]   Li T Y, Cheng L, Yan S B, Sun L J, Yao X, Yoshida Y and Ikuta H 2010 Growth and superconductivity of REBCO bulk processed by a seed/buffer layer/precursor construction *Supercond. Sci. Technol.* **23**

[24]   Kim C J, Lee J H, Park S D, Jun B H, Han S C and Han Y H 2011 Y2BaCuO5 buffer block as a diffusion barrier for samarium in top seeded melt growth processed YBa2Cu3O7-y superconductors using a SmBa2Cu3O7-d seed *Supercond. Sci. Technol.* **24**

[25]   Zhou D F, Xu K, Hara S, Li B Z, Deng Z G, Tsuzuki K and Izumi M 2012 MgO buffer-layer-induced texture growth of RE-Ba-Cu-O bulk *Supercond. Sci. Technol.* **25**

[26]   Shi Y H, Dennis A R and Cardwell D A 2015 A new seeding technique for the reliable fabrication of large, SmBCO single grains containing silver using top seeded melt growth *Supercond. Sci. Technol.* **28**

[27]   Shi Y, Babu N H and Cardwell D A 2005 Development of a generic seed crystal for the fabrication of large grain (RE)-Ba-Cu-O bulk superconductors *Supercond. Sci. Technol.* **18** L13-L6

[28]   Chen D X and Goldfarb R B 1989 KIM MODEL FOR MAGNETIZATION OF TYPE-II SUPERCONDUCTORS *Journal of Applied Physics* **66** 2489-500

[29]   Schneider C A, Rasband W S and Eliceiri K W 2012 NIH Image to ImageJ: 25 years of image analysis *Nature Methods* **9** 671